Real Time Visualization of Protein Kinase Activity in Living Cells*⑤

Ren-Hwa Yeh, Xiongwei Yan, Michael Cammer, Anne R. Bresnick‡, and David S. Lawrence§

*From the Department of Biochemistry, The Albert Einstein College of Medicine of Yeshiva University,
Bronx, New York 10461-1602*

A library of fluorescently labeled protein kinase C (PKC) peptide substrates was prepared to identify a phosphorylation-induced reporter of protein kinase activity. The lead PKC substrate displays a 2.5-fold change in fluorescence intensity upon phosphorylation. PKC activity is readily sampled in cell lysates containing the activated PKCs. Immunodepletion of conventional PKCs from the cell lysate eliminates the fluorescence response, suggesting that this peptide substrate is selectively phosphorylated by PKCα, β, and γ. Finally, living cells microinjected with the peptide substrate exhibit a 2-fold increase in fluorescence intensity upon exposure to a PKC activator. These results suggest that peptide-based protein kinase biosensors may be useful in monitoring the temporal and spatial dynamics of PKC activity in living cells.

Protein kinases, as well as the signal transduction pathways in which they participate, are now recognized to be medicinally attractive targets of opportunity (1–4). Inhibitors of the protein kinase family not only hold great promise as therapeutic agents but are also of profound utility in the characterization of signaling pathways (5). The direct visualization of protein kinase activity in living cells would provide a genuine assessment of the efficacy and selectivity of these inhibitors in a physiological setting. In addition, the ability to visualize the activity of a protein kinase in real time would furnish a direct measurement of the activation of specific signaling pathways in response to extracellular stimuli. A variety of different strategies have been described to assess protein kinase activity in cell-based systems. Ng *et al.* (6) reported the detection of phosphorylated (activated) protein kinase C (PKC)[1] α via fluorescence energy resonance transfer using cyanine-labeled anti-phospho-PKCα and antiphospho-Thr[250] antibodies in fixed cells. In this particular case, the activity of PKCα activity is not directly measured but is inferred by detecting a functional state of the enzyme. More recently, Nagai *et al.* (7) described the imaging of cAMP-dependent protein kinase activity in cells expressing a protein composed of two green fluorescent protein variants tethered by a cAMP-dependent protein kinase activity phosphorylation site. Phosphorylation of this protein generates a 23% decrease in fluorescence energy resonance transfer between the two green fluorescent proteins. By contrast, previous attempts to obtain phosphorylation-responsive fluorescently tagged peptides have been disappointing. The phosphorylation-induced change in fluorescence intensity in these systems is modest (<20%) (8–10), and as a consequence, the use of these substrates has been limited to *in vitro* experiments with purified kinases. Nonetheless, peptide substrates possess a number of inherent advantages, including ready synthetic availability, straightforward modification with the wide array of commercially available fluorophores (see "Experimental Procedures"), and the potential for complete temporal and spatial control over both when and where the substrate is phosphorylated (11–17). We describe herein a conceptually different, library-based approach for the construction and identification of peptide-based reporters of protein kinase activity. The lead fluorophore-tagged peptide from this library displays a phosphorylation-induced change in fluorescence that is an order of magnitude greater than previously described fluorophore-bearing peptide/protein substrates of protein kinases. Indeed, this lead compound serves as an effective fluorescent sensor of protein kinase activity in both cell lysates and living cells.

EXPERIMENTAL PROCEDURES
General

All chemicals were obtained from Aldrich, except for [γ-^{32}P]ATP (PerkinElmer Life Sciences), bovine serum albumin, protease and phosphatase inhibitors (Sigma), protected amino acid derivatives and Rink resin (Advanced ChemTech), antibodies (Santa Cruz Biotechnology), and Liquiscint (National Diagnostics). The α-, βII-, and γ-isoforms of protein kinase C were purchased from Panvera.

Peptide and Library Synthesis

Peptides and peptide libraries were synthesized using protocols analogous to those described previously (24).

Preparation of NBD (7-nitrobenz-2-oxa-1,3-diazole)-NH-Ser-Phe-Arg$_4$-Lys-amide **2**—A standard Fmoc/benzotriazol-1-yloxy-tris(dimethylamino)phosphonium hexafluorophosphate (Bop) peptide synthesis protocol was employed to synthesize this peptide on the Rink resin via an automated peptide synthesizer. Each amino acid was attached according to the following program (for a 2-g resin scale): (*a*) 3 × 30 ml of CH$_2$Cl$_2$; (*b*) 1 × 20 ml of 30% piperidine in CH$_2$Cl$_2$ (1 min); (*c*) 1 × 30 ml of 30% piperidine in CH$_2$Cl$_2$ (20 min); (*d*) 2 × 30 ml of CH$_2$Cl$_2$; (*e*) 1 × 30 ml of isopropyl alcohol; (*f*) 3 × 30 ml of CH$_2$Cl$_2$; (*g*) 1 × 30 ml of four equivalents of *N*-methyl morpholine in CH$_2$Cl$_2$; (*h*) three equivalents of Fmoc-protected amino acid, Bop, hydroxybenzotriazole, and six equiv-

---

⑤ The on-line version of this article (available at http://www.jbc.org) contains a description of the complete library of 417 compounds as well as a video file that shows four cells, microinjected with peptide **2**, responding to a TPA stimulus.

‡ To whom correspondence may be addressed: Dept. of Biochemistry, The Albert Einstein College of Medicine of Yeshiva University, 1300 Morris Park Ave., Bronx, NY 10461-1602. Tel.: 718-430-2741; Fax: 718-430-8565; E-mail: bresnick@aecom.yu.edu.

§ To whom correspondence may be addressed: Dept. of Biochemistry, The Albert Einstein College of Medicine of Yeshiva University, 1300 Morris Park Ave., Bronx, NY 10461-1602. Tel.: 718-430-8641; Fax: 718-430-8565; E-mail: dlawrenc@aecom.yu.edu.

[1] The abbreviations used are: PKC, protein kinase C; Bop, benzotriazol-1-yloxy-tris(dimethylamino)phosphonium hexafluorophosphate; Fmoc, 9-fluorenylmethoxycarbonyl; HPLC, high performance liquid chromatography; NBD, 7-nitrobenz-2-oxa-1,3-diazole; TPA, 12-*O*-tetradecanoyl phorbol-13-acetate; Pipes, 1,4-piperazinediethanesulfonic acid.

alents of *N*-methyl morpholine in 30 ml of CH$_2$Cl$_2$/*N*,*N*-dimethylform-amide (1:1) (60–90 min) (the coupling time was 90 min for all the Arg residues and 60 min for the other residues); (*i*) 3 × 30 ml of CH$_2$Cl$_2$; (*j*) 3 × 30 ml of 33% ethanol in CH$_2$Cl$_2$; (*k*) 2 × 30 ml of CH$_2$Cl$_2$. After completion of the desired amino acid sequence, the Fmoc group was removed with 30 ml of 30% piperidine (30 min), and the resulting side chain-protected species, H$_2$N-Ser(tBu)-Phe-[Arg(Mtr)]$_4$-Lys(Boc)-[Rink Resin], was treated with 10 equivalents of NBD-Cl and *N*-methyl mor-pholine in 1:1 CH$_2$Cl$_2$/*N*,*N*-dimethylformamide (2 ml) for 24 h to furnish the resin-linked NBD-modified peptide: NBD-HN-Ser(tBu)-Phe-[Arg-(Mtr)]$_4$-Lys(Boc)-[Rink Resin].

Preparation of H$_2$N-Ser-Phe-Arg$_4$-Lys(NBD)-amide **3**—The protocol employed for peptide **2** was likewise used to synthesize **3** with the following exceptions: *N*-α-Fmoc-*N*-ε-1-(4,4-dimethyl-2,6-dioxocyclohex-1-ylidene)ethyl-Lys ("Fmoc-Lys(Dde)") was used in place of Fmoc-Lys(t-Boc). Upon synthesis of the Ac-HN-Ser(tBu)-Phe-[Arg(Mtr)]$_4$-Lys(Dde)-[Rink Resin], the Dde protecting group was removed with hydrazine and the ε-amino moiety of Lys modified with NBD-Cl as described above. The NBD-peptide-Rink resins (*i.e.* **2** and **3**) were deprotected and cleaved as follows: each peptide resin (100 mg) was individually trans-ferred to a small reaction vessel containing 1 ml of a 9:1 trifluoroacetic acid/thioanisole mixture. The reaction vessel was then shaken at room temperature for 10 h. The resin was filtered under reduced pressure and then washed twice with trifluoroacetic acid. The filtrates were then combined (~5 ml), and an 8–10-fold volume of cold anhydrous ether (~50 ml) was added in a dropwise fashion. The mixture was kept at 4 °C for at least 1 h. The precipitated peptide was then collected via filtration through a fine sintered glass filter funnel under a light vacuum. The precipitate was washed with cold anhydrous ether (2 × 5 ml), dissolved in 10 ml of water, and finally lyophilized to provide the crude peptide. The peptides were then purified on a preparative HPLC using three Waters radial compression modules (25 × 10 cm) connected in series (gradient A: 0.1% trifluoroacetic acid in water; solvent B: 0.1% triflu-oroacetic acid in acetonitrile): 0–3 min (100% gradient A); a linear gradient from 3 to 20 min (75% gradient A and 25% solvent B); a steep final linear gradient to 90% solvent B for cleaning purposes). Peptides **2** and **3** were characterized by mass spectrometry.

In the case of the 417-member library, peptide **1** was cleaved from the Rink resin with 90% trifluoroacetic acid/10% thioanisole, purified by HPLC, and then separately acylated with fluorescent carboxylic and sulfonic acids (**I**), condensed with aryl aldehydes (**II**), or directly ary-lated (**III**) via nucleophilic aromatic substitution. Carboxylic, sulfonic, and related acid derivatives are as follows: fluorescamine, acridine-9-carboxylic acid, 5-dimethylamino-naphthalene-1-sulfonic acid, *N*, *N*′-diBoc-3-guanidino-naphthalene-2-carboxylic acid, 3-amino-naph-thalene-2-carboxylic acid, 1-hydroxy-naphthalene-2-carboxylic acid, 3-di-*tert*-butoxycarbonylmethylamino-naphthalene-2-carboxylic acid, isoquinoline-3-carboxylic acid, quinoline-2-carboxylic acid, quinoline-8-carboxylic acid, 6-carboxytetramethylrhodamine succinimidyl ester, and 1-(3-(succinimidyloxycarbonyl)benzyl)-4-(5-(4-methoxyphenyl) oxazol-2-yl) pyridinium bromide. Aldehydes and related derivatives are as follows: naphthalene-2,3-dicarbaldehyde/cyanide, naphthalene-2,3-dicarbaldehyde/thiourea, naphthalene-2,3-dicarbaldehyde/dimeth-oxymethyl-amine, naphthalene-2,3-dicarbaldehyde/aminoguanidine, naphthalene-2,3-dicarbaldehyde/2-amino-pyridine, 2,4-dinitro-benzaldehyde, 5-(4-dimethylamino-phenyl)-penta-2,4-dienal, bis-(2-hydroxy-phenyl)-methanone, bis-(4-hydroxy-phenyl)-methanone, 2-hydroxy-3,5-dinitro-benzaldehyde, anthracene-9-carbaldehyde, phen-anthrene-9-carbaldehyde, pyrene-1-carbaldehyde, 4-dime- thylamino-benzaldehyde, 2-hydroxy-4-diethylamine-benzaldehyde, 3-(4-di-methylamino-phenyl)-propenal, 4-methoxy-benzaldehyde, 2-hydroxyl-5-methoxy-benzaldehyde, 4-hydroxyl-benzaldehyde, 2,4-dimethoxyben-zaldehyde, 2-hydroxy-naphthalene-1-carbaldehyde, 4-nitro-benzalde-hyde, 2-nitrobenzaldehyde, 4-hydroxy-5-nitrobenzaldehyde, 2,6-dichloro-benzaldehyde, 4-styryl-benzaldehyde, and 3-phenyl-propenal. Aryl halides and related derivatives are as follows: NBD-Cl, 1-fluoro-2,4-dinitro-benzene, 6-chloro-5-nitro-quinoline, 2-chloro-5-trichloro-methyl-nicotinonitrile, 2-bromo-pyrimidine, 2-bromo-4,6-bis-(4-chloro-phenyl)-pyrimidine, 4-chloro-3,5-dinitro-benzonitrile, 2-fluoro-5-nitro-benzoic acid, 5-fluoro-2,4-dinitro-phenylamine, 1-fluoro-4-nitro-2-trifluoromethyl-benzene, 4-chloro-2,8-bis-trifluoromethyl-quinoline, 4-chloro-2-phenyl-quinazoline, and 2-chloro-3,5-dinitro-pyridine. A de-scription of the complete library of 417 compounds is available online as supplemental material.

Radioactive PKC Assay

Radioactive assays were performed in duplicate at 30 °C. The final assay volume totaled 40 μl and contained 62.5 mM HEPES (pH 7.4),

0.75 mM CaCl$_2$, 12.5 mM MgCl$_2$, 1 mM dithiothreitol, 0.5 mM EGTA, 7.5 μg/ml phosphatidylserine, 1.6 μg/ml diacylglycerol, and 10 ng of PKC. For the determination of the kinetic constants, the following concentra-tions were employed: 50 μM [γ-^{32}P]ATP (500–5000 cpm/pmol) and a substrate concentration that varied over a 10-fold range around the apparent K_m. Phosphorylation reactions were initiated by the addition of 10 μl of PKC from a stock solution (20 mM Tris-HCl at pH 7.5, 1 mM dithiothreitol, 1 mM EDTA, and 0.75 mg/ml bovine serum albumin) into 30 μl of assay buffer containing peptide substrate. Reactions were terminated after 5 min by spotting 25-μl aliquots onto phosphocellulose paper disks (2.1 cm in diameter). After 10 s, the disks were immersed in 10% glacial acetic acid and soaked with occasional stirring for at least 1 h. The acetic acid was decanted, and the disks were collectively washed with four volumes of 0.5% H$_3$PO$_4$, 1 volume of water followed by a final acetone rinse. The disks were air dried and then counted in a Beckman LS scintillation counter.

Fluorescent PKC Assay

Fluorescence assays were performed in triplicate at 30 °C and initi-ated by the addition of ATP to a 100-μl cuvette containing a 50-μl solution of PKC and peptide substrate **2**. Final conditions are as follows: 62.5 mM HEPES, pH 7.4, 3 mM MgCl$_2$, 0.3 mM CaCl$_2$, 0.1 mM EGTA, 1 mM dithiothreitol, 0.5 μg/ml phosphatidylserine, 0.1 μg/ml diacylglyc-erol, 1 mM ATP, and 13 nM PKC. After the addition of ATP, the solution was gently mixed, and the time-dependent change in fluorescent inten-sity (excitation, 520 nm; emission, 560 nm) was continuously monitored with a Photon Technology QM-1 spectrofluorimeter.

Preparation of Mitotic Cell Extracts

HeLa cells were synchronized for 16 h in the presence of 250 ng/ml nocodazole, and mitotic cells were collected by selective detachment. Nocodazole was removed prior to lysis by washing the cells two times with 10 ml of ice-cold phosphate-buffered saline (1.5 mM KH$_2$PO$_4$, 8 mM Na$_2$HPO$_4$/7 H$_2$O, 2.6 mM KCl, 137 mM NaCl). The cells were then resuspended in a lysis buffer containing 50 mM Pipes, pH 7.3, 5 mM MgCl$_2$, 0.2 mM EGTA, 1 M glycerol, 1 mM dithiothreitol, 0.5% Triton X-100, 1 mM phenylmethylsulfonyl fluoride, 10 μg/ml each of chymo-statin, leupeptin, and pepstatin and a 1:100 dilution of phosphatase inhibitor mixture 1 (microcystin LR, cantharidin, and (−)-*p*-bromotet-ramisole) and phosphatase inhibitor mixture 2 (sodium vanadate, so-dium molybdate, sodium tartrate, and imidazole) (Sigma). The lysates were clarified by centrifugation at 4 °C for 5 min at 16,000 × *g*, and the concentration of the supernatant was determined using the Bio-Rad protein assay (Bio-Rad Laboratories). The supernatant was diluted with dilution buffer (50 mM Tris, pH 7.5, 10 mM MgCl$_2$, 0.2 mM EGTA, 2 mM dithithreitol, 10 μg/ml each of chymostatin, leupeptin, and pep-statin, and phosphatase inhibitor mixtures 1 and 2 as described above) to a final concentration of 4 mg/ml.

PKC Activity in HeLa Cell Lysates

The PKC assay was initiated via the addition of 10 μl of HeLa mitotic lysate to a cuvette containing a preincubated (30 °C) 110-μl assay solution containing (final concentration) 10 μM peptide **2**, 10 mM ATP, 750 μM CaCl$_2$, 12.5 mM MgCl$_2$, 500 μM EGTA, 1 mM dithiothreitol, 7.5 μg/ml phosphatidylserine, 1.6 μg/ml diacylglycerol in 20 mM Tris at pH 7.5. The time-dependent change in fluorescent intensity (excitation, 520 nm; emission, 560 nm) was continuously monitored with a Photon Technology QM-1 spectrofluorimeter. The conventional PKCs α, β, and γ were immunodepleted from the HeLa cell lysate via (i) preclearance with protein A-Sepharose, (ii) incubation with the monoclonal cPKC antibody PKC(MC5) (Santa Cruz Biotechnology), (iii) addition of pro-tein A-Sepharose and subsequent centrifugation, and (iv) repetition of steps iii and iv. Protein A-Sepharose was used for mock immunode-pleted lysates. The absence of PKCs α, β, and γ was confirmed by Western blot analysis using antibodies targeted against the individual isoforms (Santa Cruz Biotechnology).

Microinjection Studies

Subconfluent, serum-starved (24 h), HeLa cells were cultured on 22-mm coverslips in Dulbecco's modified Eagle's medium in a humidi-fied atmosphere containing 5% CO$_2$. The NBD-containing peptide **2** (200 μM) in 50 mM Tris-HCl, pH 7.2, was prefiltered through a 0.22-μm filter. Microinjections were performed with an Eppendorf (Brinkman Instruments, Westbury, NY) 5246 microinjection apparatus mounted on the microscope inside the environmental chamber. We estimate a 10-fold dilution of the peptide upon microinjection from the equation for volume (*V*) flow through a capillary tube as shown in Eq. 1.

$$\left(\frac{V}{t} = \frac{\pi p r^4}{8l\eta}\right) \tag{Eq. 1}$$

where p is the difference in pressure at the ends of the tube (290 hPa), r is the radius (0.05 μm), l is the length (10 μm) of the tube, η is the viscosity of the injected solution (0.69 $\times$ 10^{-2} g/cm-sec), and t is the total injection time (0.3 s). The average volume of a fibroblast was taken as 2 picoliters (18). TPA (1 μM) was added to the media following microinjection to stimulate PKC activity. Time-lapse images were collected with 2 $\times$ 2 binning using a Photometrics (Tuscon, Az) Sensys cooled CCD camera mounted on an Olympus IX 70 inverted microscope (Melville, NY) with a PlanApo 40X N. A. 0.75 objective Ludl shutters (Hawthorne, NY) and a filter set with an excitation wavelength of 460–500 nm and an emission wavelength of 510–560 nm. Images were collected at 30-s intervals (300-ms exposure time). Fluorescence intensity measurements were corrected using values from a standard photobleaching curve generated from control experiments with microinjected HeLa cells that had not been treated with TPA. Analysis of cell intensities over time was conducted using I. P. Lab and Microsoft Excel (Redmond, OR). For experiments with the PKC inhibitor, the bisindolylmaleimide derivative GF 109203X (20 μM estimated intracellular concentration) was microinjected along with the NBD-peptide **2**.

RESULTS AND DISCUSSION

The design of a fluorescent sensor of protein kinase activity requires a substrate that contains a fluorophore positioned either near the site of phosphorylation or at a more remote site that responds to phosphorylation via a conformational change. We have shown previously that, in addition to Ser, Thr, and Tyr residues, protein kinases will catalyze the phosphorylation of a wide variety of unnatural amino acid analogs in active site-directed peptides (19–23). The synthesis of these substrates is abetted by the fact that protein kinases phosphorylate alcohol-containing residues attached to the C and/or N terminus of appropriately designed peptides. Consequently, a wide variety of Ser analogs can be easily prepared and incorporated into the peptide substrate. For example, the peptide Ser-Phe-Arg-Arg-Arg-Arg-amide contains an N-terminal serine moiety that can be readily substituted with a virtually unlimited array of functional groups. Indeed, numerous *N*-substituted analogs of this peptide serve as highly efficient substrates for the α, β, and γ isoforms of PKC (24). We reasoned that a peptide of the general structure fluorophore-Ser-Phe-Arg-Arg-Arg-Arg-amide would also function as an effective PKC substrate. The single compact fluorophore-serine residue contains a fluorescent reporter that is confined to within a few angstroms of the hydroxyl moiety, the site of imminent phosphorylation. Consequently, phosphorylation of the serine alcohol could exert a dramatic affect on the photophysical properties of the adjacent fluorophore.

The peptide H$_2$N-Ser-Phe-Arg-Arg-Arg-Arg-Lys-amide (**1**) was prepared using an Fmoc-based protocol, spatially segregated, and the free N-terminal amine was subsequently modified with an array of fluorophore-containing carboxylic acids (**I**), aromatic aldehydes (**II**), and electron-deficient aryl halides (**III**). The imines generated in **II** were also reduced to the corresponding secondary amines **IV** (NaCNBH$_3$) and transformed via aromatic nucleophilic substitution to a variety of tertiary amines **V** (Scheme I). This spatially segregated fluorophore-substituted peptide-based library contains a total of 417 distinct chemical entities and was screened for changes in fluorescence intensity in the presence of PKC and ATP under activating conditions (the structures of all 417 members of this library are provided in online supplemental material). Interestingly, the overwhelming majority (414) of these peptide-linked fluorophores displayed little (<10%) or no fluorescence change upon exposure to PKC. The obvious explanation is that phosphorylation of the peptide fails to induce the desired change in photophysical properties of the appended fluorophore. However, it is also possible that the introduction of
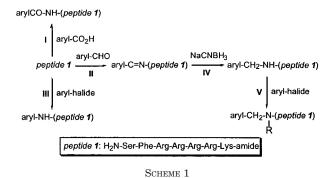

SCHEME 1

TABLE I
PKCα-catalyzed phosphorylation of selected library members

Fluorescence enhancement upon phosphorylation (% Change) was obtained by spectrofluorimetry, and K_m and k_{cat} values were acquired using the standard [γ-^{32}P]ATP radioactive assay (25).

Fluorophore-peptide	Fluorophore Reagent	% Change	K_m (μM)	k_{cat} (min^{-1})
(NBD structure) FRRRRK-amide (2)	NBD-Cl	150%	9.0 $\pm$ 1.0	380 $\pm$ 20
(Dansyl structure) FRRRRK-amide	Dansyl chloride	20%	28 $\pm$ 3	170 $\pm$ 10
(Acridine structure) FRRRRK-amide	9-Acridinecarboxylic acid	20%	13 $\pm$ 2	20 $\pm$ 2
(Cyanide/Naphthalene structure) FRRRRK-amide	Cyanide/Naphthalene -2,3-dicarbaldehyde	-	70 $\pm$ 1	220 $\pm$ 10
(Fluorescamine structure) FRRRRK-amide	Fluorescamine	-	280 $\pm$ 60	25 $\pm$ 4

fluorophores, at various sites along the peptide framework, interferes with PKC-catalyzed phosphorylation. We viewed the latter possibility as unlikely, particularly for simple *N*-monosubstituted peptides since we found previously that PKC will phosphorylate peptides containing a wide variety of structurally diverse functionality attached at and/or near the phosphorylatable serine moiety (24). Nevertheless, we evaluated in-depth a few representative members of the library (Table I). The NBD derivative **2** displays the greatest change in fluorescence intensity. By contrast, the dansyl and acridine derivatives exhibit phosphorylation-induced changes in fluorescence that are an order of magnitude less than that of NBD. The corresponding fluorescamine-treated peptide displays no fluorescence change as does the naphthalene-2,3-dicarbaldehyde/cyanide-treated species. Is the poor fluorescence response to PKC/ATP due to the fact that these peptides serve as poor PKC substrates? We addressed this question by obtaining the PKCα-catalyzed K_m and V_{max} values using the [γ-^{32}P]ATP radioactive method (25). As is clear from Table I, all five peptides are reasonably effective substrates for PKCα.

The NBD-substituted peptide was subsequently examined in greater detail. The C-terminal-positioned Lys moiety allowed us to compare fluorescence changes in response to phosphorylation as a function of NBD position (peptides **2** and **3**; Scheme II) relative to the serine moiety. We initially assessed the
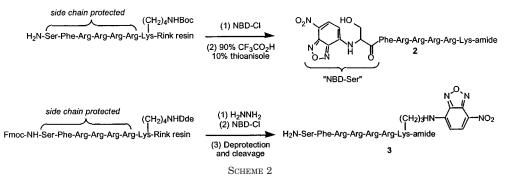
Scheme 2 (top reaction):

side chain protected

H$_2$N-Ser-Phe-Arg-Arg-Arg-Arg-Lys-Rink resin, (CH$_2$)$_4$NHBoc

(1) NBD-Cl
(2) 90% CF$_3$CO$_2$H 10% thioanisole

→ Phe-Arg-Arg-Arg-Arg-Lys-amide **2**

"NBD-Ser"

Scheme 2 (bottom reaction):

side chain protected

Fmoc-NH-Ser-Phe-Arg-Arg-Arg-Arg-Lys-Rink resin, (CH$_2$)$_4$NHDde

(1) H$_2$NNH$_2$
(2) NBD-Cl
(3) Deprotection and cleavage

→ H$_2$N-Ser-Phe-Arg-Arg-Arg-Arg-Lys-amide (CH$_2$)$_4$HN—...—NO$_2$ **3**

SCHEME 2

TABLE II

Kinetic constants associated with the phosphorylation of peptides 2 and 3 by recombinant human PKCs α, β, and γ

Substrate	Assay	Kinetic constants	PKCα	PKCβ	PKCγ
NBD-SFR$_4$K (**2**)	Radioactive	K_m (μM)	9.0 ± 1.0	9.2 ± 0.4	5.0 ± 1.0
		k_{cat} (min^{-1})	380 ± 20	180 ± 10	210 ± 20
		k_{cat}/K_m (min^{-1} μM^{-1})	42 ± 5	23 ± 2	42 ± 9
	Fluorescence	K_m (μM)	29 ± 3	27 ± 4	30 ± 5
		k_{cat} (min^{-1})	170 ± 30	94 ± 9	190 ± 40
		k_{cat}/K_m (min^{-1} μM^{-1})	5.9 ± 1	3.5 ± 0.6	6.3 ± 1.7
SFR$_4$K(ε-NBD) (**3**)	Radioactive	K_m (μM)	19 ± 1	Not determined	Not determined
		k_{cat} (min^{-1})	210 ± 10		
		k_{cat}/K_m (min^{-1} μM^{-1})	11 ± 1		
	Fluorescence	K_m (μM)			
		k_{cat} (min^{-1})		No Fluorescence Intensity Change	
		k_{cat}/K_m (min^{-1} μM^{-1})			

efficacy of **2** and **3** as PKC substrates using the radioactive ATP assay (25). Both peptides serve as efficient substrates for pure recombinant PKCα, β, and γ with K_m and k_{cat} values similar to other PKC peptide substrates (Table II).

The excitation and emission spectra of peptide **2** and its phosphorylated counterpart are furnished in Fig. 1. The most dramatic difference in the excitation spectra of the substrate and phosphorylated product is observed in the long wavelength region. Excitation of both NBD-peptide **2** and the corresponding phosphorylated derivative at 460 nm (λ_{max}) furnished a greater than 2-fold emission enhancement (>100%) in favor of the phosphorylated peptide (Fig. 1*B*). In addition, we found that excitation at a longer wavelength (520 nm) produced an even larger (2.5-fold) relative enhancement in the emission intensity of the NBD fluorophore bound to the phosphorylated peptide. By contrast, we failed to detect any change in fluorescence intensity following phosphorylation of peptide **3**. The k_{cat} and K_m values determined via spectrofluorometry are modestly different from those acquired by the corresponding radioactive method (Table II). These differences may reflect the slightly different conditions used in these assays, which were optimized to enhance fluorescence intensity changes (spectrofluorometric assay) or k_{cat}/K_m (radioactive assay). We note that the variance between the kinetic constants generated by these two different assays is small and that, using either assay, peptide **2** exhibits favorable properties as a PKC substrate for the α, β, and γ isoforms.

Several laboratories have reported the up-regulation of PKC activity during mitosis (26–29). Indeed, we have recently shown that PKC mediates the phosphorylation of the regulatory light chain of myosin II during mitosis (30). Consequently, we examined the ability of peptide **2** to report PKC activity in mitotic lysates from HeLa cells. Crude mitotic cell extracts were prepared as described previously (30), and the PKC assay was initiated via addition of the cell lysate to an assay buffer containing **2**. As shown in Fig. 2, a linear increase in fluorescence intensity is observed in the first 10 min following the addition of the cell lysate, which plateaus at ~1.7-fold above background. The protein kinase inhibitor staurosporine blocks the increase in fluorescence intensity observed upon mitotic

cell lysate addition. Staurosporine (31), like many protein kinase inhibitors (32, 33), targets a variety of protein kinases. Consequently, from these experiments, it is not clear whether the staurosporine-induced block of fluorescence is due to the inhibition of PKC activity or the inhibition of other protein kinases that also catalyze the phosphorylation of peptide **2**.

We addressed whether the peptide substrate **2** is selective for the conventional PKCs by immunodepleting the mitotic cell lysates of PKCs α, β, and γ using a commercially available antibody that recognizes all three PKC isoforms. Depletion of the individual α, β, and γ isoforms from the cell lysate was confirmed by immunoblot analysis using isoform-specific antibodies (shown for PKCα in Fig. 3). Analogous Western blots were performed for the β and γ PKC isoforms as well (data not shown). The immunodepleted lysate (Fig. 3, *lane 3*) was examined for PKC activity in the fluorescence assay. We did not detect any change in fluorescence intensity over the course of 1 h (Fig. 2, *plot D*). The latter observation is consistent with the notion that the fluorescence enhancement observed with crude mitotic lysates is due to PKC. It is unlikely that a protein kinase downstream from PKC is responsible for the observed enhancement in fluorescence since this putative downstream kinase would have already been activated in the cell lysate prior to immunodepletion of the conventional PKCs.

Given the enzymological and photophysical behavior displayed by peptide **2**, we examined the *in vivo* visualization of PKC activity in live cells. Serum-starved HeLa cells were microinjected with the NBD-modified peptide, and the cells were subsequently exposed to TPA, a tumor-promoting phorbol ester that potently and specifically activates PKC (34). A change in fluorescence intensity is evident within 4 min of TPA exposure and significantly so by 8 min (Fig. 4). Fig. 4 serves as a link to a video file that is available online. In this video, four cells that have been microinjected with peptide **2** are shown responding in a fluorescently sensitive fashion to the TPA stimulus. A comparison of the curves generated in the lysate (Fig. 2) and live cell (Fig. 5) assays demonstrate that both curves display an essentially linear increase in fluorescence intensity within the first 10 min of exposure to activated PKC followed by a plateau
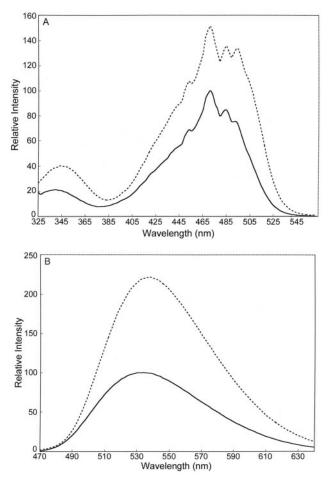
FIG. 1. **Excitation (*A*) and emission (*B*) spectra of the substrate peptide 2 (*solid line*) and the phosphorylated species 3 (*dashed line*).** The emission spectra in *curve B* were produced by exciting the NBD fluorophore at its λ_{max} (460 nm).
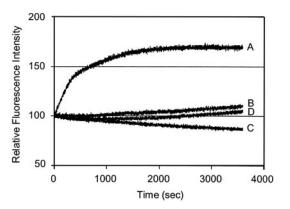

FIG. 2. **PKC activity in mitotic HeLa cell lysates.** The PKC assay was initiated by the addition of the lysate to the assay buffer. Fluorescence change as a function of incubation time in the presence of cell lysate (*A*), in the absence of cell lysate (*B*), in the presence of cell lysate and 4.5 μM staurosporine (*C*), and in the presence of cPKC immunodepleted cell lysate (*D*).

phase shortly thereafter. The overall enhancement in fluorescence intensity displayed by peptide **2** in living cells is 2-fold, whereas the cell lysate-based experiments furnish an overall 1.7-fold increase in fluorescence. In an additional series of experiments, the NBD-peptide PKC substrate was co-injected with the known PKC inhibitor, GF 109203X (35). This inhibitor effectively blocks the TPA-induced enhancement in cellular fluorescence. Although the K_i value for GF 109203X is in the low nanomolar range, micromolar concentrations of GF
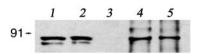

FIG. 3. **Immunodepletion of PKC from mitotic cell lysates.** Western blot analysis was performed with anti-PKCα antibody. *Lane 1*, crude cell lysate. *Lane 2*, cell lysate precleared with Protein-A-Sepharose. *Lane 3*, cell lysate following immunodepletion of PKC. *Lane 4*, PKC immunoprecipitate following initial treatment of the mitotic cell lysate. *Lane 5*, PKC immunoprecipitate following a second treatment of the mitotic cell lysate.
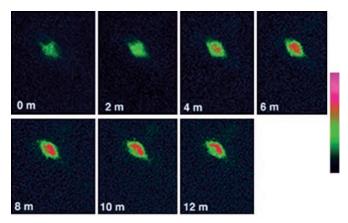

FIG. 4. **TPA-induced time-dependent change in fluorescence intensity in HeLa cells with peptide 2.** Time-lapse images of TPA-stimulated HeLa cells microinjected with peptide **2**. These images serve as a link to a video file available online that shows four cells, microinjected with peptide **2**, responding to a TPA stimulus.
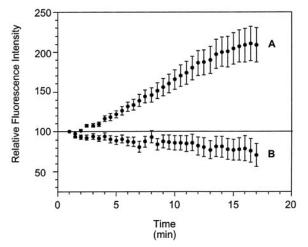

FIG. 5. **TPA-induced time-dependent change in fluorescence intensity in HeLa cells containing the microinjected peptide 2 (*A*) and the microinjected peptide 2 in the presence of 20 μM GF 109203X (*B*).** Time-lapse fluorescence intensity measurements of TPA-stimulated HeLa cells microinjected with peptide **2**. Combined data from 16 cells is furnished in *segment A*, and combined data from 14 cells is provided in *segment B*.

109203X were used to block *in vivo* PKC activity due to the presence of high intracellular levels of ATP.

In summary, a fluorescent substrate for PKC has been constructed using a strategy that positions the reporter group directly on the residue undergoing phosphorylation. A library of fluorescently labeled PKC peptide substrates was prepared. The lead derivative displays a phosphorylation-induced fluorescence change that allows the visualization of real time PKC activity in both cell lysates and living cells. Furthermore, immunodepletion experiments suggest that the fluorescently tagged peptide is selectively, if not exclusively, phosphorylated by the conventional PKCs. The PKC biosensor strategy out-

Fluorescent Probes of PKC Activity

lined herein takes advantage of the ease with which peptides can be modified to create libraries of structurally altered analogs. However, the inherent synthetic mutability of peptides is not just limited to library construction. For example, it may be possible to simultaneously monitor more than one protein kinase by affixing fluorophores with distinct photophysical properties to the N or C termini of appropriately designed active site-directed peptides. Furthermore, there exists the potential for temporal and spatial control over when and where the substrate is phosphorylated via the preparation of "caged" analogs (11–14). These possibilities, as well as others, are currently under investigation.

REFERENCES

1. Sebolt-Leopold, J. S. (2000) *Oncogene* **19,** 6594–6599
2. Popoli, M., Mori, S., Brunello, N., Perez, J., Gennarelli, M., and Racagni, G. (2001) *Pharmacol. Ther.* **89,** 149–170
3. Agarwal, R. (2000) *Biochem. Pharmacol.* **60,** 1051–1059
4. Senderowicz, A. M. (2001) *Leukemia* (Baltimore) **15,** 1–9
5. Lawrence, D. S., and Niu, J. (1998) *Pharmacol. Ther.* **77,** 81–114
6. Ng, T., Squire, A., Hansra, G., Bornancin, F., Prevostel, C., Hanby, A., Harris, W., Barnes, D., Schmidt, S., Mellor, H., Bastiaens, P. I. H., and Parker, P. J. (1999) *Science* **283,** 2085–2089
7. Nagai, Y., Miyazaki, M., Aoki, R., Zama, T., Inouye, S., Hirose, K., Iino, M., and Hagiwara, M. (2000) *Nat. Biotechnol.* **18,** 313–316
8. Post, P. L., Trybus, K. M., and Taylor, D. L. (1994) *J. Biol. Chem.* **269,** 12880–12887
9. McIlroy, B. K., Walters, J. D., and Johnson, J. D. (1991) *Anal. Biochem.* **195,** 148–152
10. Bowman, B. F., Peterson, J. A., and Stull, J. T. (1992) *J. Biol. Chem.* **267,** 5346–5354
11. Wood, J., Koszelak, M., Liu, J., and Lawrence, D. S. (1998) *J. Am. Chem. Soc.* **120,** 7145–7146
12. Marriot, G., and Walker, J. W. (1999) *Trends Plant Sci.* **4,** 330–334
13. Curley, K., and Lawrence, D. S. (1999) *Pharmacol. Ther.* **82,** 347–354
14. Walker, J. W., Gilbbert, S. H., Drummond, R. M., Yamada, M., Sreekumar, R., Carraway, R. E., Ikebe, M., and Fay, F. S. (1998) *Proc. Natl. Acad. Sci. U. S. A.* **95,** 1568–1573
15. Pirrung, M. C., Drabik, S. J., Ahamed, J., and Ali, H. (2000) *Bioconjugate Chem.* **11,** 679–681
16. Tatsu, Y., Shigeri, Y., Ishida, A., Kameshita, I., Fujisawa, H., and Yumoto, N. (1999) *Bioorg. Med. Chem. Lett.* **9,** 1093–1096
17. Pan, P., and Bayley, H. (1997) *FEBS Lett.* **405,** 81–85
18. Kislauski, E. H., Zhu, X.-C., and Singer, R. (1997) *J. Cell Biol.* **136,** 1263–1270
19. Lee, T. R., Niu, J., and Lawrence, D. S. (1995) *J. Biol. Chem.* **270,** 5375–5380
20. Kwon, Y.-G., Mendelow, M., and Lawrence, D. S. (1994) *J. Biol. Chem.* **269,** 16725–16729
21. Lee, T. R., Mendelow, M., Srinivasan, J., Kwon, J.-G., and Lawrence, D. S. (1993) *J. Am. Chem. Soc.* **115,** 9888–9891
22. Yan, X., Lawrence, D. S., Corbin, J. D., and Francis, S. H. (1996) *J. Am. Chem. Soc.* **117,** 11684–11685
23. Lee, T. R., Niu, J., and Lawrence, D. S. (1994) *Biochemistry* **33,** 4245–4250
24. Yan, X., Curley, K., and Lawrence, D. S. (2000) *Biochem. J.* **349,** 709–715
25. Glass, D. B., Masaracchia, R. A., Feramisco, J. R., and Kemp, B. E. (1978) *Anal. Biochem.* **87,** 566–575
26. Goss, V. L., Hocevar, B. A., Thompson, L. J., Stratton, C. A., Burns, D. J., and Fields, A. P. (1994) *J. Biol. Chem.* **269,** 19074–19080
27. Collas, P. (1999) *J. Cell Sci.* **112,** 977–987
28. Passalacqua, M., Patrone, M., Sparatore, B., Pedrazzi, M., Melloni, E., and Pontremoli, S. (1999) *FEBS Lett.* **453,** 249–253
29. Takai, Y., Ogawara, M., Tomono, Y., Moritih, C., Imajoh-Ohmi, S., Tsutsumi, O., Taketani, Y., and Inagaki, M. (1996) *J. Cell Biol.* **133,** 141–149
30. Varlamova, O., Spektor, A., and Bresnick, A. R. (2001) *J. Muscle Res. Cell Motil.* **22,** 243–250
31. Way, K. J., Chou, E., and King, G. L. (2000) *Trends Pharmacol. Sci.* **21,** 181–187
32. Lingameneni, R., Vysotskaya, N., Duch, D. S., and Hemmings, H. C., Jr. (2000) *FEBS Lett.* **473,** 265–268
33. Davies, S. P., Reddy, H., Caivano, M., and Cohen, P. (1999) *Biochem. J.* **351,** 95–105
34. Gschwendt, M., Kittstein, W., and Marks F. (1991) *Trends Biochem. Sci.* **16,** 167–169
35. Goekjian, P. G., and Jirousek, M. R. (1999) *Curr. Med. Chem.* **6,** 877–903